

Contiguous phosphorylated and non-phosphorylated domains along axonal neurofilaments

Anthony Brown

Neurobiology Program, Department of Biological Sciences, Ohio University, Athens, OH 45701, USA
(e-mail: browna1@ohiou.edu)

Accepted 1 December 1997; published on WWW 27 January 1998

SUMMARY

I have investigated the phosphorylation state of the medium molecular mass neurofilament protein (NF-M) along axonal neurofilaments. Cultured embryonic sensory neurons were treated with non-ionic detergent to cause the cytoskeletal polymers to splay apart from each other. Neurofilaments were visualized by double-label immunofluorescence microscopy and the proportion of their length that stained with various NF-M antibodies was determined using digital image analysis techniques. Monoclonal antibody RMO255, which binds to NF-M independently of phosphorylation state, stained an average of 98% of the neurofilament length. In contrast, monoclonal antibody RMO55, which binds specifically to a phosphorylated epitope on NF-M, stained some neurofilaments completely, some not at all, and some along part of their length. These partly stained neurofilaments exhibited single or multiple discrete segments of staining along their length separated by segments that were unstained. The average proportion of the neurofilament length that stained with this antibody was lowest proximally (12-22%, $n=3$) and increased along the axon to reach a maximum distally (58-87%, $n=3$). A converse pattern (77-87% proximally and 2-9% distally, $n=3$) was

observed for neurons stained with monoclonal antibody FNP7, which binds specifically to a non-phosphorylated epitope in both NF-M and the high molecular mass neurofilament protein, NF-H. Analysis of the staining of individual neurofilaments revealed a bimodal frequency distribution in which neurofilaments were more likely to be phosphorylated along either all or none of their length than along part of their length. These observations indicate that: (a) phosphorylated and non-phosphorylated neurofilaments can coexist side-by-side in these axons, (b) neurofilaments can be composed of single or multiple contiguous phosphorylated and non-phosphorylated epitope domains along their length, (c) the proportion of the neurofilament length that is phosphorylated at these epitopes increases along the axon in a proximal-to-distal manner, and (d) the pattern of phosphorylation is non-random, generating populations of phosphorylated and non-phosphorylated neurofilaments and discrete phosphorylated and non-phosphorylated domains along individual neurofilaments.

Key words: Neurofilament, Phosphorylation, Axonal cytoskeleton

INTRODUCTION

Neurofilaments are neuronal intermediate filaments that function to impart mechanical integrity to nerve cells and their processes and to increase the cross-sectional area of axons, thereby influencing the axonal conduction velocity (Cleveland et al., 1991). The identity and stoichiometry of the polypeptides that comprise these cytoskeletal polymers varies greatly according to phylogenetic source, neuronal type and developmental age. In mammals, neurofilaments are generally considered to be composed of three principal polypeptides called NF-L (low molecular mass; 66 kDa), NF-M (medium molecular mass; 95-100 kDa) and NF-H (high molecular mass; 110-115 kDa), known collectively as the 'neurofilament triplet' (for reviews, see Lee and Cleveland, 1996; Shaw, 1991). In common with other intermediate filament proteins, each triplet polypeptide consists of a central alpha-helical 'rod' domain flanked by a short N-terminal 'head' domain and a longer C-

terminal 'tail' domain. The different sizes of the triplet proteins are due principally to differences in the lengths of the tail domains. The long tail domains of the two higher molecular mass neurofilament triplet proteins form radial projections called side-arms that project from the filament backbone at regular intervals and may function to keep adjacent filaments at 'arm's length' thereby maximizing the space-filling properties of these polymers in axons (Eagles et al., 1990).

Both the head and tail domains of the neurofilament triplet proteins are modified *in vivo* by phosphorylation (for review, see Nixon and Sihag, 1991). Radioisotopic pulse-labeling studies have demonstrated that some of these phosphates are subject to turnover during axonal transport and therefore the phosphorylation state of each neurofilament protein *in vivo* is considered to represent a dynamic balance between the actions of kinases and phosphatases (Nixon and Lewis, 1986). Little is known about the phosphatases that act on neurofilaments but one candidate is protein phosphatase 2A, which can

dephosphorylate sites within both the head and tail domains of the neurofilament polypeptides *in vitro* (Saito et al., 1995; Veeranna et al., 1995). Phosphorylation of the head and tail domains is better understood and appears to be mediated by multiple and distinct classes of protein kinases. For example, studies *in vitro* have shown that the head domains contain sites that can be phosphorylated by protein kinase A, protein kinase C and calcium/calmodulin-dependent protein kinase, whereas the tail domains contain sites that can be phosphorylated by casein kinase I and proline-directed kinases such as cdk5 and mitogen-activated protein kinase (MAP kinase) (for review, see Pant and Veeranna, 1995). In the case of NF-M and NF-H, most of the phosphates are located in the long carboxy-terminal tail domains (Chin et al., 1989; Julien and Mushynski, 1983) and most of these phosphorylation sites share the consensus sequence X(S/T)PX which identifies them as targets of proline-directed kinases (Elhanany et al., 1994; Xu et al., 1992).

Phosphorylation of the head and tail domains of neurofilament proteins has distinct effects on the structure and organization of neurofilaments in axons. For example, site-specific phosphorylation of the head domain appears to regulate filament stability and subunit assembly properties (Hisanaga et al., 1990, 1994; Saito et al., 1995). In contrast, phosphorylation of the tail domains of NF-M and NF-H appears to have more general effects on the physical properties of these domains, possibly favoring a more extended conformation for the neurofilament sidearms so as to increase the space-filling properties of the polymers (de Waegh et al., 1992; Nixon et al., 1994), or possibly modulating their interactions with neighboring neurofilaments (Gotow and Tanaka, 1994; Gotow et al., 1994) or microtubules (Hisanaga and Hirokawa, 1990; Hisanaga et al., 1993).

An interesting feature of neurofilament protein phosphorylation is that the extent of phosphorylation varies both spatially and temporally in a well-defined manner. For example, immunocytochemical studies with antibodies specific for phosphorylated and non-phosphorylated epitopes in the tail domains of NF-M and NF-H have shown that poorly phosphorylated forms always precede more heavily phosphorylated forms during neuronal development and this is thought to correlate with the radial growth of axons as they mature (Carden et al., 1987; Foster et al., 1987). In addition to these developmental changes, there are also marked spatial differences in the phosphorylation state of neurofilaments within neurons. Specifically, at all stages of development neurons contain poorly phosphorylated neurofilaments in their cell bodies, dendrites and proximal axons and more extensively phosphorylated neurofilaments at distal locations in their axons (Carden et al., 1987; Lee et al., 1987; Sternberger and Sternberger, 1983). Furthermore, several laboratories have reported a proximal-to-distal gradient of increasing phosphorylation for neurofilament proteins along axons, both in culture (Bennett et al., 1984; Benson et al., 1996) and *in vivo* (Archer et al., 1994; Szaro et al., 1989). However, the functional significance of these spatial and temporal differences in neurofilament phosphorylation state has not been established.

To better understand the process of neurofilament phosphorylation in axons, I have investigated the distribution of phosphorylated epitopes along single neurofilaments in cultured neurons. To visualize single axonal neurofilaments, I

have taken advantage of the splayed axonal cytoskeleton preparation in which the cytoskeletal polymers splay apart from each other during detergent extraction allowing individual neurofilaments and microtubules to be resolved from each other by conventional immunofluorescence light microscopy (Brown, 1997; Brown et al., 1993). The data presented here confirm the existence of a proximal-to-distal gradient of increasing neurofilament phosphorylation along axons. In addition, the data demonstrate that neurofilaments in these neurons can be composed of contiguous phosphorylated and non-phosphorylated epitope domains that are distributed non-randomly and that phosphorylated and non-phosphorylated segments of neurofilament polymer can coexist side-by-side. Thus the gradient of phosphorylation along these axons appears to reflect an increase in the proportion of the total polymer that is phosphorylated rather than a uniform and continuous increase in phosphorylation across all polymers.

MATERIALS AND METHODS

Cell culture

Primary cultures of dissociated neurons were established from the dorsal root ganglia of E16.5 rat embryos and maintained in a medium based on the N2 formulation of Bottenstein and Sato (1979), supplemented with 50 ng/ml 2.5S nerve growth factor, 10% adult rat serum and 0.5% hydroxypropylmethylcellulose, as described by Brown (1997). All studies were performed between 24 and 46 hours after the time of plating.

Detergent treatment, fixation and immunostaining

Axonal neurofilaments were visualized using the splayed axonal cytoskeleton preparation described by Brown (1997). To induce neurofilament splaying, cells were treated with 0.5% saponin in a solution composed of 60 mM NaPipes, 25 mM NaHepes, 10 mM NaEGTA, 2 mM MgCl₂, 0.19 M NaCl, pH 6.9. Subsequently the cells were fixed with 4% (w/v) formaldehyde, extracted further with a solution containing 1% Triton X-100 and 0.3 M NaCl, and processed for double-label immunofluorescence microscopy as described by Brown (1997). All primary antibodies were provided by Dr Virginia Lee of the University of Pennsylvania. NF-M was visualized with mouse monoclonal antibody RMO55, which is specific for phosphorylated NF-M (NF-M P⁺, Lee et al., 1987), mouse monoclonal antibody RMO255, which is specific for NF-M but binds independently of phosphorylation state (NF-M Pi, Lee et al., 1987), and mouse monoclonal antibody FNP7, which binds specifically to the non-phosphorylated forms of NF-M and NF-H (NF-M/H P⁻). RMO255 and RMO55 were raised in mice against purified rat NF-M (Lee et al., 1987). RMO55 binds to a phosphorylated epitope in the tail domain of rat NF-M (Virginia Lee, personal communication). RMO255 binds to an epitope in the tail domain of rat NF-M between residues 761 and 845 (Harris et al., 1991) which is a region of NF-M that does not appear to be phosphorylated *in vivo* (Xu et al., 1992). FNP7 was raised to a non-phosphorylated synthetic peptide containing the sequence KSPVPKSPVEE (Virginia Lee, personal communication), which is located between residues 603 and 613 in the tail domain of rat NF-M. This sequence contains two phosphorylation sites, both of which can be phosphorylated *in vivo* (Xu et al., 1992). NF-L was visualized using a rabbit polyclonal antiserum (NFLAS) which binds independently of phosphorylation state (NF-L Pi; Trojanowski et al., 1989). This antiserum was raised against a 20 amino acid synthetic peptide identical to the extreme C terminus of human NF-L (Trojanowski et al., 1989). The primary antibodies were visualized with FITC-conjugated donkey anti-rabbit IgG (minimum cross-reactivity to mouse, rat and other species;

Jackson Immunoresearch, West Grove, PA) and indocarbocyanine (Cy3)-conjugated donkey anti-mouse IgG (minimum cross-reactivity to rabbit, rat and other species; Jackson Immunoresearch).

Immunoblotting

The specificity of the monoclonal and polyclonal antibodies was confirmed by immunoblotting using rat neurofilament proteins. A crude preparation of rat neurofilaments was obtained from adult rat spinal cords essentially as described by Lee et al. (1987). The proteins were separated by SDS-PAGE on 7.5% polyacrylamide gels using a Hoefer Tall Mighty Small gel apparatus (Pharmacia Biotech, Piscataway, NJ) and transferred onto nitrocellulose (Nitrobind® membrane, 0.45 µm pore size, Micron Separations Inc., Westborough, MA) using a Multiphor II NovaBlot semi-dry blotting apparatus (Pharmacia Biotech). Transferred proteins were visualized by staining a strip of the nitrocellulose blot with a solution of Ponceau S in 5% acetic acid (Sigma Chemical Co., St Louis, MO). For immunostaining, strips of the nitrocellulose blot were blocked with a 5% (w/v) solution of Carnation brand non-fat dry milk in Tris buffered saline (TBS; 50 mM Tris-HCl, 138 mM NaCl, 2.7 mM KCl, pH 7.4) and then incubated in primary antibody diluted 1:1,000 in TBS containing 1% normal goat serum (Jackson Immunoresearch). Unbound primary antibody was rinsed off with TBS containing 0.1% Tween-20 (Sigma) and the blot strips were then incubated in secondary antibody (goat anti-mouse IgG or goat anti-rabbit IgG, conjugated to horseradish peroxidase) at a dilution of 1:50,000 in TBS containing 4% normal goat serum (Jackson Immunoresearch). Unbound secondary antibody was rinsed off with TBS containing 0.1% Tween-20 and the bound antibody was visualized on the blot strips using diaminobenzidine/NiCl₂ as the peroxidase substrate.

Enzymatic dephosphorylation

To test the dependence of antibody binding on phosphorylation state by immunoblotting, the neurofilament proteins were dephosphorylated enzymatically by treating the nitrocellulose blots with 1.5 units/ml alkaline phosphatase (Type III-L, purified from *Escherichia coli*, Sigma) in dephosphorylation buffer (50 mM Tris-HCl, 138 mM NaCl, 2.7 mM KCl, 1 mM ZnSO₄, pH 8.0) for 18 hours at room temperature (Carden et al., 1985; Sternberger and Sternberger, 1983). Subsequently the alkaline phosphatase was removed by rinsing with 400 mM sodium phosphate, 100 mM NaCl, 50 mM NaEDTA, pH 7.2. The dishes were then processed for immunoblotting as described above. To test the dependence of antibody binding on phosphorylation state by immunofluorescence microscopy, neurofilaments in splayed axonal cytoskeletons were dephosphorylated enzymatically in situ by treating fixed cultures with 1.5 units/ml alkaline phosphatase in dephosphorylation buffer (see above) for 18 hours at 37°C (Foster et al., 1987). Subsequently the alkaline phosphatase was removed by rinsing with TBS containing 10 mM NaEDTA and then with TBS alone. The dishes were then processed for immunofluorescence as described above.

Microscopy and image acquisition

The stained cells were observed by epifluorescence microscopy using a Nikon Diaphot 300 microscope (Nikon Inc., Melville, NY) and the following oil immersion objectives: Zeiss ×25/0.8NA Plan Neofluar (Carl Zeiss, Inc., Thornwood, NY), Nikon CF N ×40/1.0 NA Plan Apo, and Nikon CF N ×100/1.4 NA Plan Apo. Digital images were acquired using a CH250 cooled CCD camera equipped with a Kodak KAF 1400 chip (Photometrics Ltd, Tucson, AZ). All image acquisition, processing and analysis was performed with an Apple Macintosh computer using Oncor-Image (formerly BDS-Image) digital image processing and analysis software (Version 2.0, Oncor Inc., Gaithersburg, MD). A more detailed description of these procedures is given by Brown (1997). Digital images were prepared for publication in Adobe Photoshop 4.0 (Adobe Systems Inc., San Jose, CA).

Construction of montages

To analyze neurofilament lengths, a series of overlapping images of the NF-L fluorescence were acquired at low magnification (×25 objective) for the entire axon of interest. A second series of non-overlapping images of both the NF-L and NF-M fluorescence were then acquired at high magnification (×100 objective) at regularly spaced intervals along the axon. To create a montage of the neuron, the low magnification images of the NF-L fluorescence were subjected to a threshold operation to obtain a binary image of the axon, inverted to produce a black image against a white background, and then arranged by alignment of the regions of overlap using Canvas software (Deneba Systems, Inc., Miami, FL). The precise location of the fields photographed at high magnification was determined by applying a 4-fold reduction to these ×100 images and then superimposing them on the low magnification montage. The length of the axon was determined in Oncor-Image by tracing its medial axis starting at the geometric center of the cell body and ending at the tip of the growth cone. The distance of each high magnification image field from the cell body was calculated as the distance along the axon from the geometric center of the cell body to the mid-point of the axon in that image.

Method of analysis

The proportion of each neurofilament that stained with a particular NF-M antibody was measured using the Oncor-Image software and programs written using the Oncor-Image programming language (Fig. 1). Single neurofilaments were selected for measurement using the image of the NF-L fluorescence because NF-L is known to be present in all neurofilaments in vivo (Ching and Liem, 1993; Lee et al., 1993). Neurofilaments were excluded from these analyses if they could not be traced unambiguously for at least 0.1 µm, if they were bundled with other filaments, or if they were separated completely from the axonal neurofilament bundle so that both ends were visible. To measure neurofilament lengths, the images of the NF-L and NF-M fluorescence (Fig. 1A,C) were subjected to a thresholding operation to create a binary image of the splayed axonal cytoskeletons and these binary images were then skeletonized to yield single pixel-width lines corresponding to the medial axes of the selected neurofilaments (Fig. 1B,D, superimposed in 1E to aid comparison). The length of each line was measured using programs written in the Oncor-Image programming language and these measurements were used to calculate the percentage of the length of each neurofilament that was stained with the NF-M antibody.

Pseudocolor imaging

To visualize the distribution of the NF-M antibodies along individual neurofilaments, artificial color was applied to the images of the NF-L and NF-M antibody fluorescence in Adobe Photoshop (Adobe Systems Inc., San Jose, CA) and the two images were superimposed digitally to create a dual color image. The artificial colors were chosen to resemble the actual colors of fluorescein and rhodamine fluorescence so that the resulting pseudocolor images had the appearance of conventional dual-channel immunofluorescence in which regions of overlap between the two channels appear orange. No registration of the superimposed images was necessary because they were found to be in register to within one pixel width (for a discussion of image registration see Brown et al., 1992).

RESULTS

Characterization of antibodies

The specificity of the antibodies used in this study was confirmed by immunoblotting using a crude preparation of rat neurofilaments. To test the dependence of antibody binding on

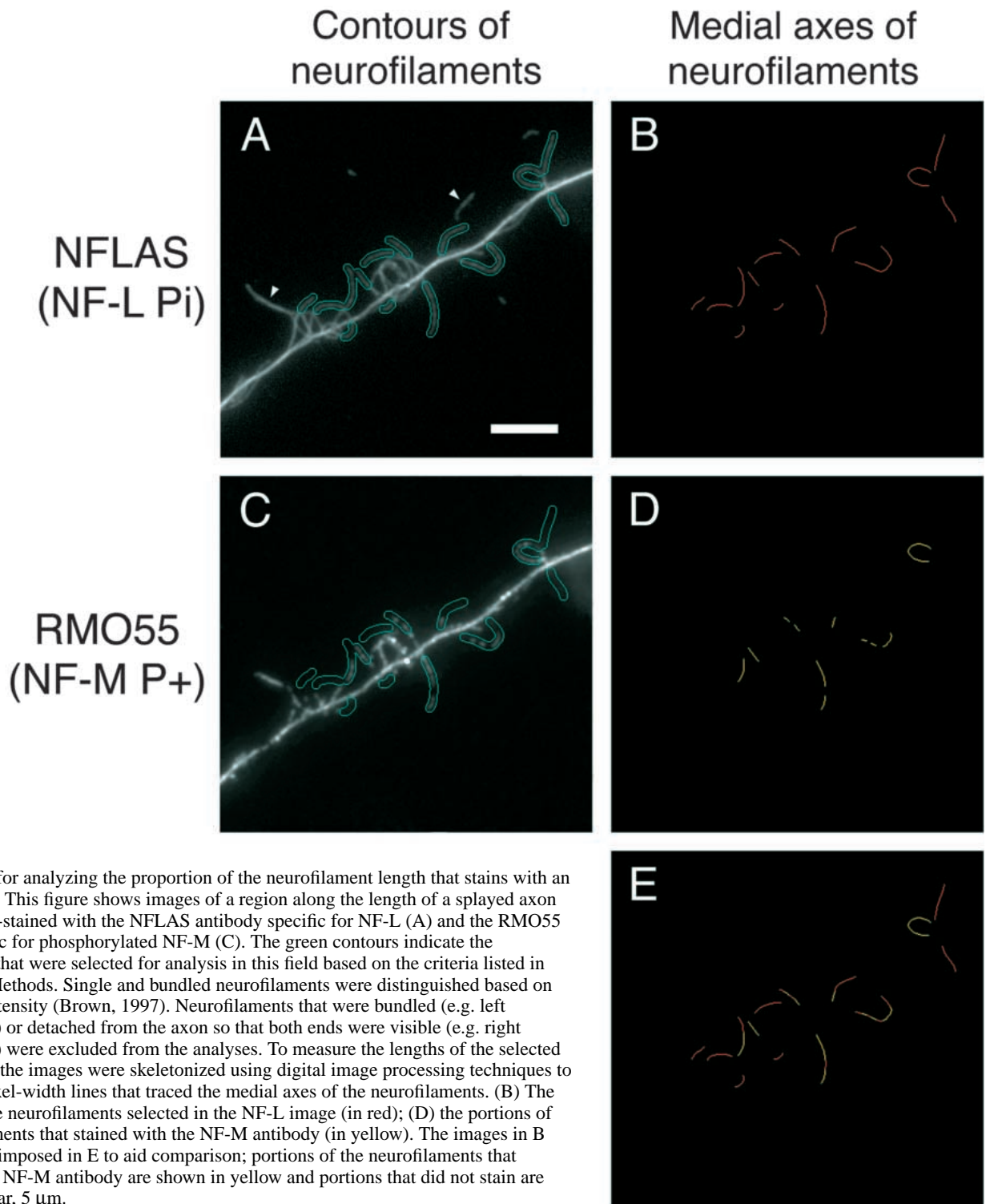


Fig. 1. Method for analyzing the proportion of the neurofilament length that stains with an NF-M antibody. This figure shows images of a region along the length of a splayed axon that was double-stained with the NFLAS antibody specific for NF-L (A) and the RMO55 antibody specific for phosphorylated NF-M (C). The green contours indicate the neurofilaments that were selected for analysis in this field based on the criteria listed in Materials and Methods. Single and bundled neurofilaments were distinguished based on their staining intensity (Brown, 1997). Neurofilaments that were bundled (e.g. left arrowhead in A) or detached from the axon so that both ends were visible (e.g. right arrowhead in A) were excluded from the analyses. To measure the lengths of the selected neurofilaments, the images were skeletonized using digital image processing techniques to create single pixel-width lines that traced the medial axes of the neurofilaments. (B) The skeletons for the neurofilaments selected in the NF-L image (in red); (D) the portions of these neurofilaments that stained with the NF-M antibody (in yellow). The images in B and D are superimposed in E to aid comparison; portions of the neurofilaments that stained with the NF-M antibody are shown in yellow and portions that did not stain are shown in red. Bar, 5 μ m.

phosphorylation state, I dephosphorylated the neurofilament proteins after blotting by incubating the nitrocellulose strips with alkaline phosphatase (see Materials and Methods). This dephosphorylation procedure does not result in the usual mobility shift for NF-M and NF-H (Georges and Mushynski, 1987) because the phosphatase treatment is performed after the polypeptides have been separated by SDS-PAGE.

Fig. 2A shows the protein composition of the crude rat

neurofilament preparation. The minor bands indicated by the open arrowheads represent hypo-phosphorylated NF-M and NF-H, which are present in small quantities in rat spinal cord tissue (Lee et al., 1986, 1987). The rabbit antiserum, NFLAS, bound to NF-L in its native phosphorylation state (Fig. 2B) and its binding was not affected significantly by enzymatic dephosphorylation (Fig. 2C). NFLAS did not bind to NF-M or NF-H, though it did bind to an unknown minor component with

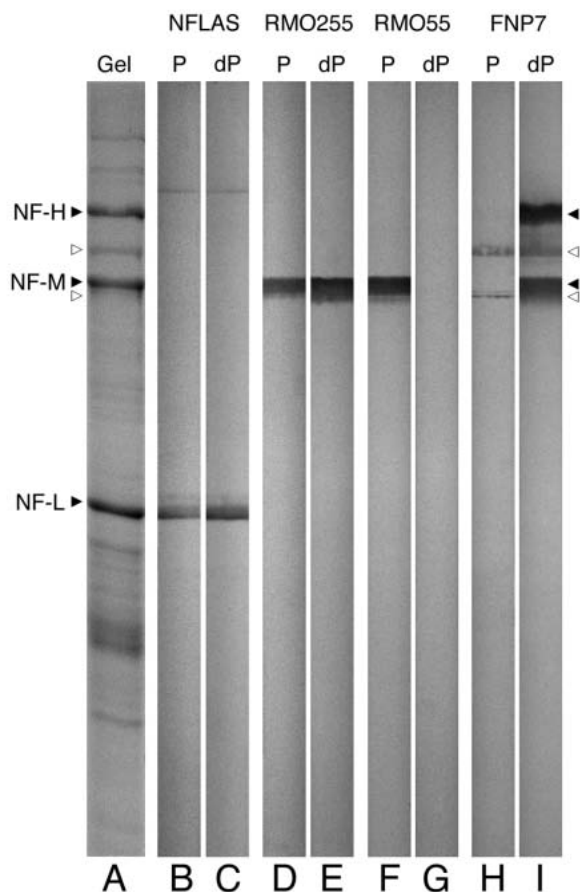


Fig. 2. Characterization of antibodies by immunoblotting. (A) The neurofilament proteins separated by SDS PAGE. (B-I) Nitrocellulose blot strips stained with NFLAS (B,C), RMO255 (D,E), RMO55 (F,G) and FNP7 (H,I). (B,D,F,H) The blot strips marked P represent the untreated (phosphorylated) neurofilament preparation; (C,E,G,I) the blot strips marked dP represent the same protein preparation after enzymatic dephosphorylation with alkaline phosphatase prior to immunostaining. The closed arrowheads mark the location of the neurofilament triplet proteins (NF-H, NF-M and NF-L) and the open arrowheads mark the location of endogenous hypophosphorylated NF-M and NF-H, which have a higher mobility by SDS-PAGE (see text).

a higher apparent molecular mass than NF-H in both the untreated and dephosphorylated preparations. These data are consistent with previous reports that the NFLAS antiserum is specific for NF-L and binds independently of phosphorylation state (Trojanowski et al., 1989).

Monoclonal antibodies RMO255 and RMO55 both bound specifically to untreated (i.e. phosphorylated) NF-M (Fig. 2D,F) but RMO255 also bound to enzymatically dephosphorylated NF-M (Fig. 2E) whereas RMO55 did not (Fig. 2G). These data indicate that RMO55 binds specifically to a phosphorylated epitope on NF-M, whereas RMO255 binds to NF-M independently of its phosphorylation state, and this is consistent with previous reports for these antibodies (Harris et al., 1991; Lee et al., 1987). The monoclonal antibody FNP7 did not bind detectably to phosphorylated NF-M or NF-H (closed arrowheads) but it did stain the small amount of endogenous hypophosphorylated NF-M and NF-H present in the rat

neurofilament preparation (Fig. 2H; see open arrowheads). After enzymatic dephosphorylation, staining of NF-M and NF-H by FNP7 was greatly increased (Fig. 2I; see closed arrowheads), indicating that this antibody binds specifically to a non-phosphorylated epitope present in both NF-M and NF-H.

To confirm that the NF-M antibodies exhibit the same phosphorylation dependence in the immunofluorescence protocol, I treated splayed axonal cytoskeletons (see below) with alkaline phosphatase and then visualized the neurofilaments by immunofluorescence microscopy. Fig. 3 shows the results of such an experiment in which the neurofilaments were double-stained with the NFLAS (NF-L P⁻) and RMO55 (NF-M P⁺) antibodies. For this experiment, I focused on the distal end of the axon where neurofilament phosphorylation is most extensive (see below). The NFLAS antiserum stained neurofilaments uniformly and continuously in both the untreated and dephosphorylated preparations (compare Fig. 3A,B). In contrast, the RMO55 antibody stained the majority of the neurofilaments in untreated preparations but did not stain any of the neurofilaments after enzymatic dephosphorylation (compare Fig. 3C,D). This confirms that the RMO55 antibody binds to neurofilaments in a phosphorylation-dependent manner in the immunofluorescence protocol, consistent with the data obtained by immunoblotting.

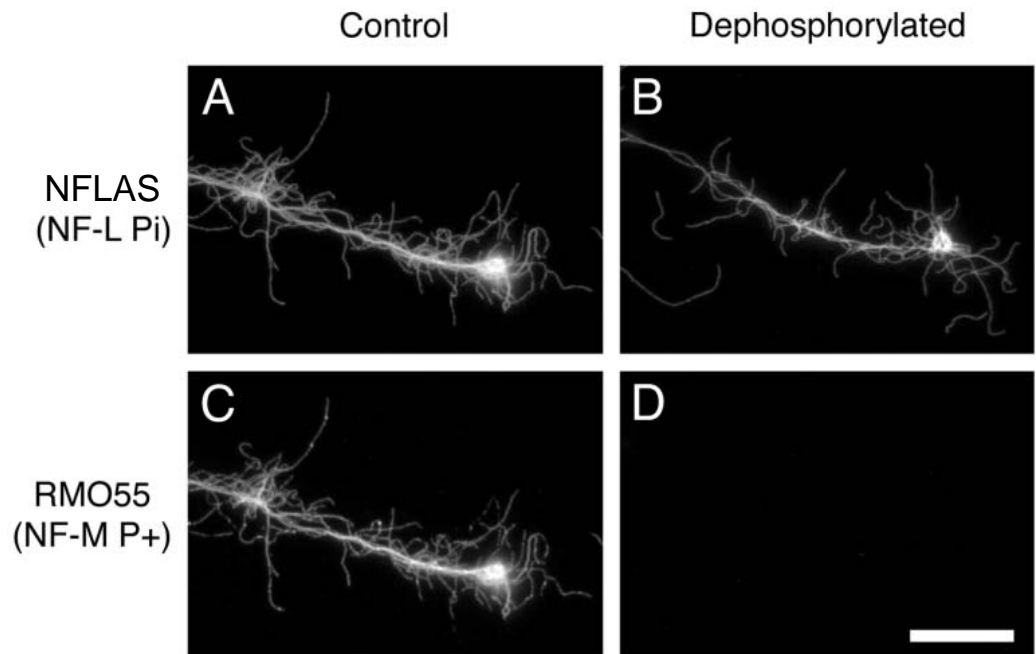
Analysis of neurofilament phosphorylation state along axons

Dissociated neurons plated at low density typically extended two or three axons that grew at rates of approximately 30-50 $\mu\text{m}/\text{hour}$ and exhibited little branching. The nine axons analyzed in this study ranged from 24 to 46 hours in age and from 679 μm to 2,304 μm in length. Axonal neurofilaments were visualized by treatment of the neurons with detergent under conditions that cause the cytoskeletal polymers to splay apart from each other (see Materials and Methods). The splayed preparations were then fixed and double-stained with a rabbit polyclonal antiserum specific for NF-L and one of three mouse monoclonal antibodies specific for different phosphorylation states of NF-M.

To analyze the phosphorylation state of NF-M along the splayed axons, images were acquired at regular intervals from the cell body to the growth cone using a $\times 100$ objective magnification. Neurofilaments were identified based on their staining for NF-L and the proportion of their length that stained with the NF-M antibodies was measured as described in Materials and Methods. Fig. 4 shows a montage of a typical neuron and the locations of six $\times 100$ images that were acquired along one of its axons. The number and length of the neurofilaments that could be analyzed in each image field was dependent on the extent of splaying. In the present study, the mean neurofilament length analyzed was 2.2 μm (minimum=0.1, maximum=27 μm , $n=2115$) and the mean number of neurofilaments analyzed per axon was 235 (minimum=111, maximum=622 μm , $n=9$). Though the extent of splaying generally varied along the length of individual axons, quantitative comparison of the data pooled from nine different axons revealed no significant difference between the extent of splaying proximally versus distally (data not shown).

Fig. 5 shows the results of my analyses for three different NF-M antibodies. Each point in these graphs represents the percentage of the total neurofilament length that was labeled

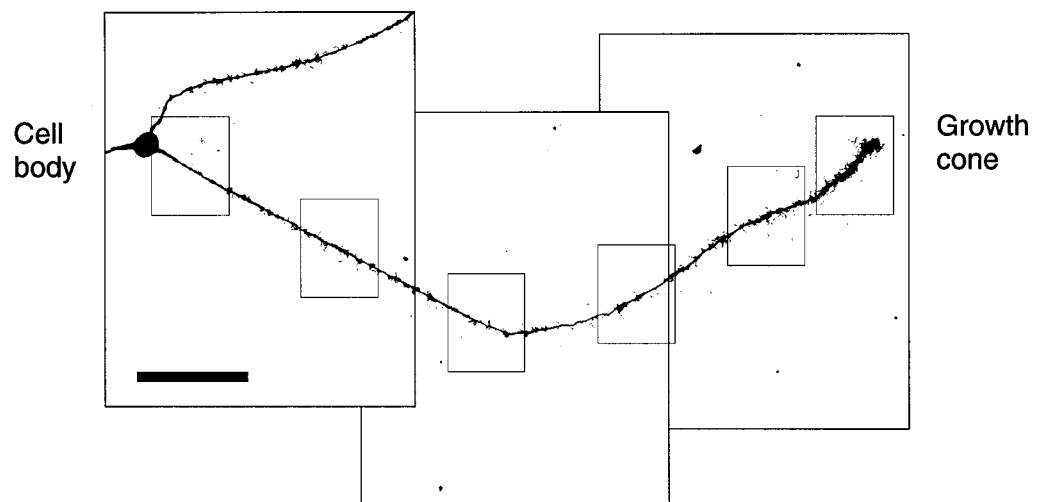
Fig. 3. Binding of RMO55 antibody is abolished by neurofilament dephosphorylation. (A and C) Images of the distal end of an axon double-stained with the NFLAS antiserum (NF-L Pi), which binds specifically to NF-L independently of its phosphorylation state, and the RMO55 antibody (NF-M P+), which binds specifically to phosphorylated NF-M. (B and D) Images of the distal end of an axon double-stained with the same antibodies after enzymatic dephosphorylation. I selected the distal end of the axon for this figure because the neurofilaments in this region stain with RMO55 along most of their length (see text). The NFLAS antiserum stained both untreated (A) and dephosphorylated (B) neurofilaments, confirming that the binding of this antibody is independent of phosphorylation state. In contrast, the RMO55 antibody stained untreated (C) but not dephosphorylated (D) neurofilaments, confirming that the binding of this antibody is dependent on phosphorylation state. Bar, 15 μ m.



with the NF-M antibody in a single $\times 100$ image field. Fig. 5A-C shows the data for three axons that were stained with monoclonal antibody RMO255 (NF-M Pi), which binds to NF-M independently of its phosphorylation state (the data in Fig. 5A correspond to the cell illustrated in Fig. 4). The average proportion of the neurofilament length that labeled with this antibody varied between 93% and 100% for the $\times 100$ image fields analyzed along these three axons (mean = $98 \pm 2.5\%$, $n=18$). These data indicate that NF-M is present along almost the entire length of the neurofilaments in these axons. Fig. 5D-F shows the data for three axons that were stained with RMO55 (NF-M P+), which binds specifically to a phosphorylated epitope on NF-M. In contrast to RMO255, a significant proportion of the neurofilaments in each axon did not stain with

RMO55. Furthermore, the proportion of the neurofilament length that was phosphorylated at the RMO55 epitope was lowest proximally and increased along the axon in a proximal-to-distal manner. Specifically, the proportion of the neurofilament length that was stained within a single $\times 100$ field varied from 12 to 22% proximally (within 174 μ m of the cell body) and increased in a proximal-to-distal manner, reaching a maximum value of 58-87% distally (within 161 μ m of the growth cone). The converse pattern was observed for FNP7 (NF-M/H P-), which binds specifically to a non-phosphorylated epitope present in both NF-M and NF-H (Fig. 5G-I). Specifically, the proportion of the neurofilament length that was stained by FNP7 within a single $\times 100$ image field varied from 77 to 87% proximally (within 79 μ m of the cell

Fig. 4. Montage of a neuron. The cell shown here was processed for immunostaining after 24 hours in culture, as described in Materials and Methods. This cell has three axons, only one of which is shown in its entirety. The axons have a tattered appearance because the cell was treated with detergent prior to fixation to cause the neurofilaments to splay apart from each other. The montage was created from three overlapping images of the fluorescence acquired using a $\times 25$ objective magnification and the outlines of these images are shown by the three large rectangles. The six smaller rectangles correspond to fields that were acquired for analysis using a $\times 100$ objective magnification. Bar, 100 μ m.



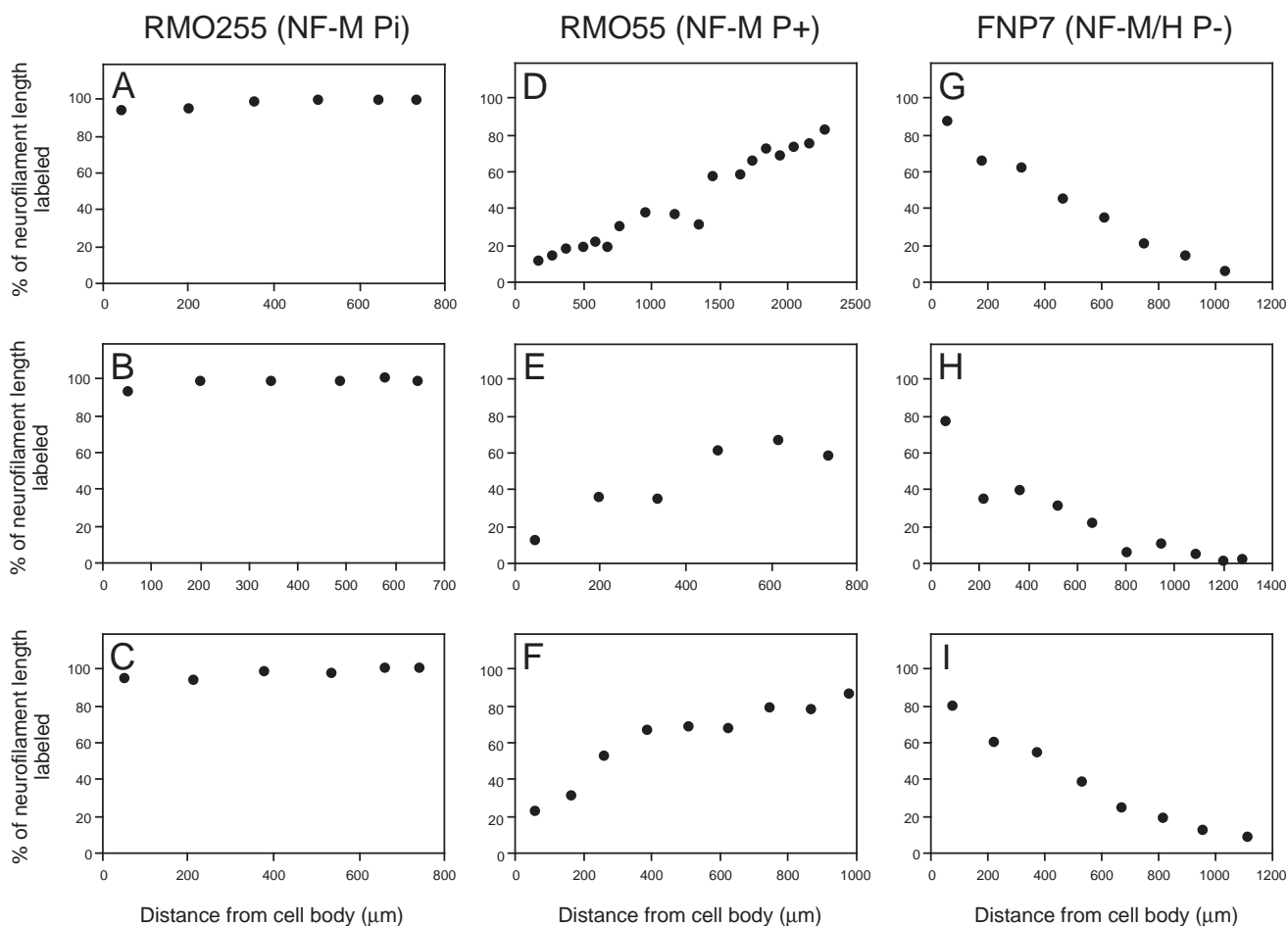


Fig. 5. Analysis of NF-M phosphorylation state along axons. Each graph shows the proportion of the neurofilament length that stained with the NF-M antibody plotted against distance along the axon, measured from the cell body towards the growth cone. Each point in the graphs represents the proportion of the total neurofilament length that stained with the NF-M antibody within a single field acquired using a $\times 100$ objective. Three examples are shown for each NF-M antibody. (A-C) The data for the RMO255 antibody, which binds independently of phosphorylation state (NF-M Pi). (C-F) The data for the RMO55 antibody, which binds to a phosphorylated epitope on NF-M (NF-M P+). (G-I) The data for the FNP7 antibody, which binds to a non-phosphorylated epitope on NF-M and NF-H (NF-M/H P-). These data show that essentially all of the neurofilaments contain NF-M but that the proportion of this protein that is phosphorylated increases along these axons in a proximal-to-distal manner.

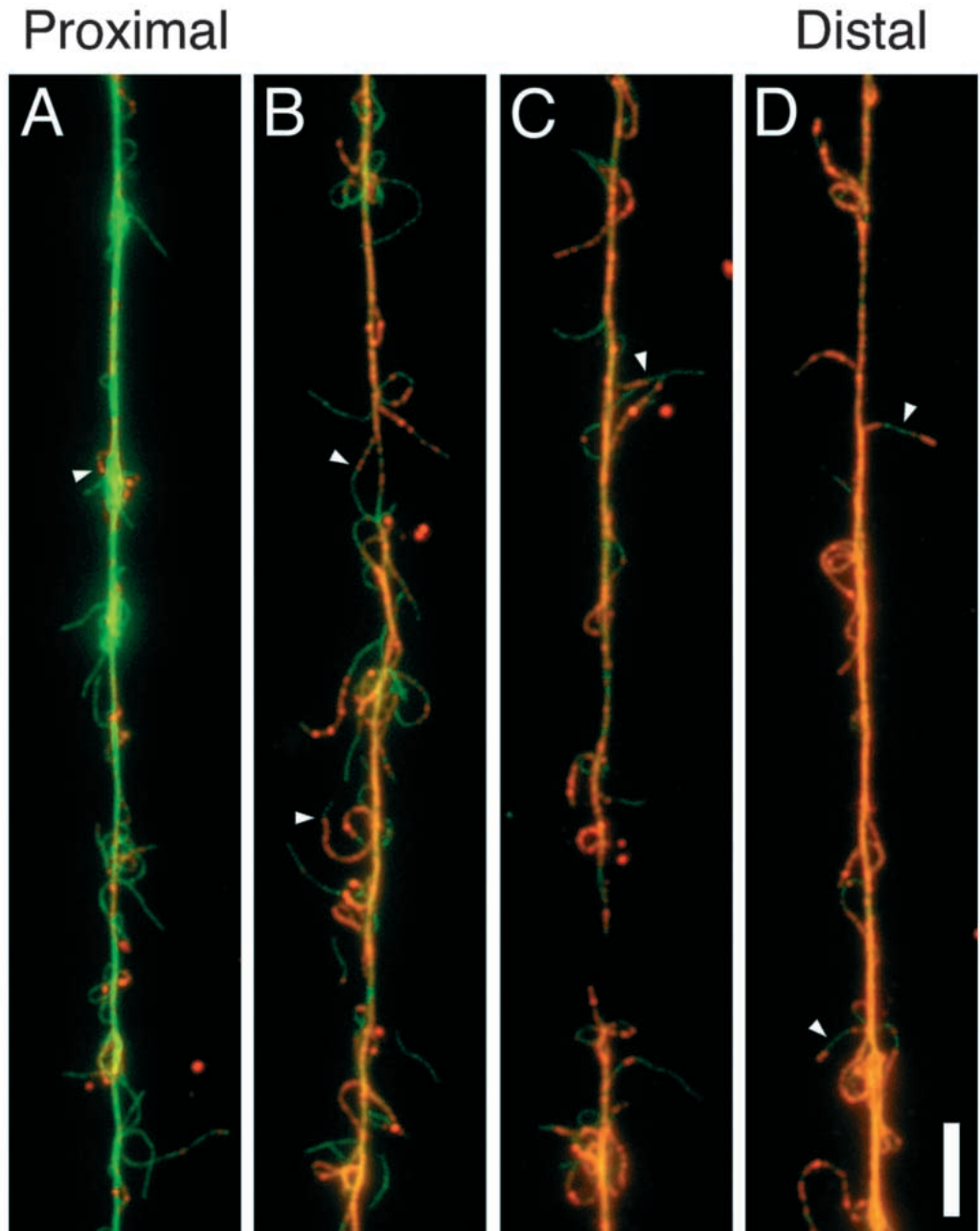
body) and decreased in a proximal-to-distal manner, reaching a minimum value of 2-9% distally (within 35 μm of the growth cone). In spite of the cross-reactivity of the FNP7 antibody for NF-H, its staining pattern in these experiments is most likely to be due principally to NF-M because NF-H is expressed at very low levels in these and other embryonic neurons both *in vivo* (Carden et al., 1987; Pachter and Liem, 1984; Riederer et al., 1996; Shaw and Weber, 1982) and *in culture* (Foster et al., 1987; Lee, 1985; Shaw et al., 1985). These observations demonstrate that NF-M is present in neurofilaments throughout these axons but that there is a continuous proximal-to-distal gradient in the phosphorylation of this protein at the RMO55 and FNP7 epitopes which extends along the entire axon from the cell body to the growth cone.

Analysis of neurofilament phosphorylation state along individual neurofilaments

To visualize the distribution of phosphorylated epitopes along the length of individual neurofilaments, I created dual color

images of the splayed axonal cytoskeletons by superimposition of the double-stained images of the NF-M and NF-L fluorescence. Fig. 6 shows the resulting dual color images for the RMO55 antibody (NF-M P+). Towards the proximal end of the axon, most neurofilaments that had splayed apart from the axon did not stain, though occasional short segments of staining were visible (Fig. 6A). Given that neurofilaments in these axons contain NF-M along an average of 98% of their length (see above), this staining pattern indicates that most neurofilaments in the proximal regions of these axons contain NF-M that is not phosphorylated at the RMO55 epitope. Moving distally along the axon, the number of neurofilaments that stained with RMO55 increased (Fig. 6B,C). In these medial regions of the axon, some neurofilaments were unlabeled along their entire visible length, some were labeled along their entire visible length, and some contained one or more contiguous labeled and unlabeled segments with discrete transitions between them (see arrowheads in Fig. 6B,C). Towards the distal end of the axon, most of the neurofilaments

Fig. 6. Visualization of phosphorylated NF-M along individual neurofilaments. Images of splayed axons double-stained for NF-L (NFLAS antibody; visualized with green fluorescence) and phosphorylated NF-M (RMO55 antibody; visualized with red fluorescence). Regions of the neurofilaments that contain phosphorylated NF-M stain orange due to the coincidence of the red and green light; other regions stain green. The four images shown here represent four sites along the axon, from proximal (A) to distal (D). The distance from the cell body as a percentage of the total axon length was 7% for A, 25% for B, 59% for C, and 91% for D. A is from an axon that was 736 μm long and B, C and D are from another axon that was 914 μm long. Proximally, very few neurofilaments contain phosphorylated NF-M (A). The arrowhead in A points to a short phosphorylated segment. Medially, the proportion of the neurofilaments containing phosphorylated NF-M is greater and abrupt transitions between phosphorylated and non-phosphorylated domains can be observed along single neurofilaments (e.g. arrowheads in B and C). Note that some neurofilaments contain more than one such transition along their length. Distally, the proportion of the neurofilaments that contain phosphorylated NF-M is greater still and non-phosphorylated domains along neurofilaments are few (e.g. arrowheads in D). Bar, 5 μm .

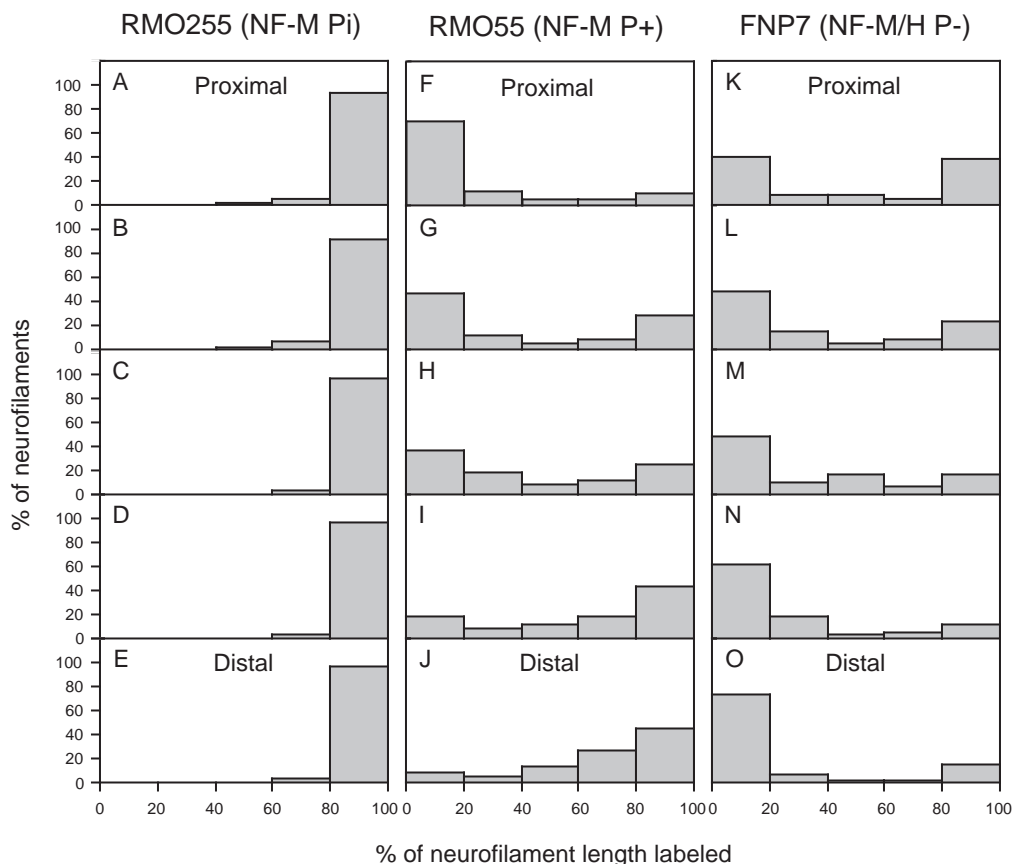


stained with RMO55 along their entire visible length, only occasionally interrupted by unstained regions. Contiguous labeled and unlabeled regions were also observed along individual neurofilaments stained with FNP7 (data not shown), but the proportion of the total neurofilament length that stained with this antibody was highest proximally and declined in a proximal-to-distal manner, consistent with the quantitative analyses shown in Fig. 5. These observations indicate that neurofilaments in these axons can consist of contiguous phosphorylated and non-phosphorylated domains along their length and that the proximal-to-distal increase in neurofilament phosphorylation demonstrated in Fig. 5 is due at least in part to an increase in the proportion of the total neurofilament length that is labeled. Interestingly, these data also show that phosphorylated and non-phosphorylated neurofilaments can

coexist side-by-side, and this is especially common in medial portions of these axons.

Close inspection of dual-color images such as those shown in Fig. 6 gave the impression that the labeling with the RMO55 and FNP7 antibodies was not random. Specifically, many neurofilaments were either completely labeled or completely unlabeled along their entire visible length. Furthermore, neurofilaments that contained both labeled and unlabeled regions generally appeared to be composed of a small number discrete labeled and unlabeled domains rather than a random punctate distribution of labeling along the filament axis. To examine this quantitatively, I analyzed the percentage labeling for individual neurofilaments in the nine axons shown in Fig. 5. To allow comparison of proximal, medial and distal regions of the axons, I subdivided each axon into five regions of equal

Fig. 7. Frequency distributions for the extent of neurofilament labeling along axons. Graphs A-E depict the data for the RMO255 (NF-M Pi) antibody, F-J for the RMO55 (NF-M P+) antibody and K-O for the FNP7 (NF-M/H P-) antibody. To obtain these data, the data from three different axons were combined for each antibody. To allow comparison of different regions along the length of the axons, each axon was subdivided into five measurement windows of equal length, extending from the cell body to the growth cone. To allow data from axons of different length to be pooled, the distance of these measurement windows from the cell body was calculated as a percentage of the axon length. The distance of these measurement windows along the axons was 0-20% (i.e. the proximal 20% of the axon length) in A, F and K, 20-40% in B, G and L, 40-60% in C, H and M, 60-80% in D, I and N, and 80-100% (i.e. the distal 20% of the axon length) in E, J and O. The average number of neurofilaments analyzed for each histogram was 141 (minimum=42, maximum=339).



length and calculated a percentage labeling frequency distribution for the neurofilaments within each region.

Fig. 7A-E shows the resulting data for the RMO255 antibody, which binds to NF-M independently of phosphorylation state (NF-M Pi). The great majority of the neurofilaments were labeled along 80-100% of their length in each axonal region, and in all cases the frequency distribution was unimodal. In contrast, the histograms for the RMO55 (NF-M P+) and FNP7 (NF-M/H P-) antibodies were bimodal with peak numbers of neurofilaments in the 0-20% and 80-100% labeling categories throughout the axon. For example, Fig. 7H shows the frequency distribution for RMO55 labeling at a medial location along the axon, mid-way between the cell body and the growth cone. Inspection of Fig. 5D-F shows that the overall percentage of the neurofilament length that stained at this medial location was 30-70% for the three axons analyzed. In spite of this, more neurofilaments were labeled along 0-20% and 80-100% of their length than in any other individual category, and neurofilament segments that were labeled along 40-60% of their length were the least numerous. In the proximal axon, the distribution was skewed to the left because most neurofilaments were completely unlabeled with RMO55 (Fig. 7F), and in the distal axon the distribution was skewed to the right because most neurofilaments were completely labeled with RMO55 (Fig. 7J). Nevertheless, even in these proximal and distal regions a bimodal distribution was still apparent. These observations indicate that neurofilaments in these axons are more likely to be phosphorylated at the RMO55 and FNP7 epitopes along either all or none of their length than along part

of their length, which implies that the kinase or kinases that phosphorylate neurofilaments at these epitopes do so in a non-random manner.

DISCUSSION

The splayed axonal cytoskeleton preparation offers a useful method for studying the post-translational modification or polypeptide composition of cytoskeletal polymers in axons using conventional immunofluorescence microscopy. In addition to the present study on axonal neurofilaments, this preparation has also been used to investigate the distribution of tyrosinated, acetylated and biotinylated tubulin along axonal microtubules (Brown et al., 1993; Li and Black, 1996; Rochlin et al., 1996; Slaughter et al., 1997). Similar information can be obtained by immunoelectron microscopy using serial reconstructions but the major advantages of the splayed axonal cytoskeleton preparation are its relative speed and simplicity, and the opportunity for quantification of staining intensity using fluorescence microscopy. The principal disadvantage of this preparation is that only those cytoskeletal polymers that separate from the axonal neurofilament bundle can be analyzed and the number and length of these polymers is dependent on the extent of splaying, which is somewhat variable (Brown, 1997). Nevertheless, individual neurofilaments in the present study could be traced unambiguously for an average length of 2 μ m and many hundreds of such segments could be analyzed along a typical axon.

To investigate the phosphorylation of axonal neurofilaments I stained splayed axonal cytoskeletons with monoclonal antibodies specific for different phosphorylation states of the medium molecular mass neurofilament protein, NF-M. To establish the dependence of antibody binding on phosphorylation state, I stained untreated and enzymatically dephosphorylated rat neurofilament proteins with these antibodies by western blotting and immunofluorescence procedures. Even though alkaline phosphatase has been used widely for this purpose, it should be noted that this enzyme may not remove all phosphates from the neurofilament polypeptides. In fact, estimates of the efficacy of dephosphorylation by alkaline phosphatase range from 49 to 99% for NF-M and NF-H in intact neurofilaments *in vitro* (Carden et al., 1985; Georges et al., 1986; Hisanaga and Hirokawa, 1989). Nevertheless, the dramatic effect that treatment with alkaline phosphatase has on the binding of RMO55 and FNP7 by immunoblotting and on the binding of RMO55 by immunofluorescence microscopy indicates that this enzyme does dephosphorylate NF-M in an effective manner, at least at the sites recognized by these antibodies.

Analysis of splayed axonal cytoskeletons stained with the RMO255 (NF-M Pi) antibody demonstrated that NF-M is coassembled with NF-L along 98% of the neurofilament length in these neurons. This is consistent with evidence that NF-L and NF-M are coexpressed during development of the rodent nervous system (Carden et al., 1987; Cochard and Paulin, 1984) and that neurofilaments are obligate heteropolymers *in vivo*, requiring the presence of NF-L and one or both of the high molecular mass proteins for filament formation (Ching and Liem, 1993; Lee et al., 1993). In contrast to RMO255, the RMO55 (NF-M P+) and FNP7 (NF-M/H P-) antibodies stained some neurofilament segments entirely, some not at all, and some along only part of their length. Neurofilaments that stained along part of their length exhibited discrete alternating stained and unstained regions with abrupt transitions between them. Since the RMO55 and FNP7 antibodies bind to NF-M in a phosphorylation-dependent manner, this indicates that neurofilament polymer in these axons can exist in phosphorylated or non-phosphorylated states at these epitopes and that single neurofilaments can contain contiguous phosphorylated and non-phosphorylated epitope domains along their length. The existence of a non-uniform distribution of phosphorylated and non-phosphorylated epitopes along axonal neurofilaments has also been reported for the high molecular mass neurofilament protein, NF-H, in the rat central nervous system using immunogold labeling in conjunction with electron microscopy (Gotow and Tanaka, 1994). Discrete labeled and unlabeled domains such as those described here were not apparent in their study but it is possible that this is due to differences between the immunofluorescence and immunogold procedures in the efficiency or sensitivity of labeling. In principle, it is possible that labeled and unlabeled domains along neurofilaments could be generated artefactually in immunostaining protocols by differential masking of epitopes. However, this seems unlikely because these domains were only observed with the phosphorylation-dependent antibodies and not with the phosphorylation-independent antibodies.

Quantitative analyses along axons demonstrated that while stained and unstained filaments were observed throughout the

axons, the average proportion of the neurofilament length that stained with the RMO55 antibody was lowest proximally and increased towards the growth cone whereas the average proportion of the neurofilament length that stained with the FNP7 antibody was highest proximally and decreased towards the growth cone. Given the specificities of these antibodies, this indicates that there is a proximal-to-distal gradient of neurofilament phosphorylation at the RMO55 and FNP7 epitopes. At medial sites along the axon, phosphorylated and non-phosphorylated segments of neurofilament polymer were intermingled, which indicates that phosphorylated and non-phosphorylated neurofilaments can coexist side-by-side within the axon.

The existence of a gradient in neurofilament phosphorylation along these axons is consistent with previous reports from a number of laboratories both in culture (Bennett et al., 1984; Benson et al., 1996) and *in vivo* (Archer et al., 1994; Szaro et al., 1989). In addition, the quantitative data presented here extend these observations by demonstrating that this gradient is not due simply to a uniform and continuous increase in the phosphorylation state of the neurofilaments along the axon. Rather, neurofilaments appear to be composed of discrete phosphorylated and non-phosphorylated domains along their length and the gradient in neurofilament phosphorylation appears to be due, at least in part, to an increase along the length of the axon in the proportion of the neurofilament length that is phosphorylated.

The existence of a proximal-to-distal gradient of phosphorylation along axons is not unique to neurofilament proteins. For example, studies on cultured neurons have demonstrated that there is a proximal-to-distal increase in the phosphorylation of the microtubule-associated protein MAP-1b along axons (Black et al., 1994) and a proximal-to-distal decrease in the phosphorylation of the microtubule associate protein tau (Mandell and Banker, 1996). One possible explanation for these proximal-to-distal gradients is the existence of parallel gradients of kinase or phosphatase activity along the axon, as suggested by Szaro et al. (1989). In the case of neurofilaments, this hypothesis is problematic because the present study shows that phosphorylated and non-phosphorylated neurofilaments can coexist within the same region of the axon. An alternative explanation is that such gradients could reflect a slow post-translational modification of these proteins during their transport along the axon. Like all axonal proteins, neurofilament proteins are synthesized in the neuronal cell body and transported into and along the axon by a process called axonal transport. Considerable evidence now indicates that neurofilament triplet proteins normally exist in a hypophosphorylated form in the soma and that phosphorylation of the tail domains is a slow post-translational modification that occurs after the neurofilament proteins have assembled into filaments and during their transit along the axon (Bennett and DiLullo, 1985; Black et al., 1986; Nixon et al., 1987; Oblinger, 1987). Therefore it is possible that the proximal-to-distal gradient of neurofilament phosphorylation along axons reflects a gradient of neurofilament age, with the youngest least phosphorylated neurofilaments located proximally, close to their site of assembly in the cell body and the oldest most extensively phosphorylated neurofilaments located distally, farthest from the cell body. However, while neurofilament age could well

be the principal determinant of the extent of neurofilament phosphorylation in isolated neurons in culture, it is likely that neurofilament phosphorylation in vivo is modulated by additional factors, such as interactions with myelinating cells (de Waegh et al., 1992; Mata et al., 1992; Nixon et al., 1994; Starr et al., 1996) and possibly other environmental cues (Landmesser and Swain, 1992).

The data presented in this paper raise a number of questions. Firstly, what is the significance of the existence of discrete phosphorylated and non-phosphorylated domains along neurofilaments? Discrete domains of post-translational modification are also observed for tyrosinated and acetylated alpha tubulin along axonal microtubules (Baas and Black, 1990; Brown et al., 1993). However, these microtubules contain a single domain that is tyrosinated tubulin poor and acetylated tubulin rich contiguous with a single domain that is tyrosinated tubulin rich and acetylated tubulin poor; multiple contiguous domains are not encountered. Furthermore, the tyrosinated tubulin rich and acetylated tubulin poor domain is always present at the distal end of the microtubule, which corresponds to the plus end in axons because of their uniform polarity orientation. Since detyrosination and acetylation are considered to be markers of older or less dynamic microtubule polymer, it has been suggested that this pattern of post-translational modification represents a snap-shot of the assembly history of the polymer, with a dynamic or more recently assembled (i.e. 'younger') plus-end domain contiguous with a less dynamic or less recently assembled (i.e. 'older') minus-end domain (Brown et al., 1993). In contrast to microtubules, neurofilaments are not known to possess any structural polarity and the data presented in this paper indicate that single neurofilaments can apparently contain more than one discrete phosphorylated segment along their length, with no apparent preference for neurofilament ends. Furthermore, there is no evidence for any relationship between the phosphorylation state of neurofilament protein tail domains and the assembly dynamics of neurofilament polymers. Therefore, while the post-translational modification of neurofilaments and microtubules is clearly a time-dependent process, it seems likely that the phosphorylated and non-phosphorylated domains along neurofilaments arise by a quite different mechanism than the domains of post-translationally modified tubulin along microtubules.

One possible explanation for the existence of discrete phosphorylated and non-phosphorylated domains along neurofilaments is that these domains reflect the random action of neurofilament kinases. To test this hypothesis, I examined the extent of labeling of individual neurofilaments with the RMO55 antibody. These analyses revealed a bimodal frequency distribution in which neurofilaments were more likely to be either poorly phosphorylated (0-20% of length labeled) or heavily phosphorylated (80-100% of length labeled) than to be phosphorylated to intermediate extents. This pattern of labeling is not consistent with a random distribution of phosphorylation sites and it suggests that the kinase or kinases that phosphorylate NF-M at the RMO55 and FNP7 epitopes do so in a non-random manner. One possibility is that these kinases exhibit a kind of spatial cooperativity, being more likely to phosphorylate these epitopes in a part of the filament that contains other phosphorylated NF-M proteins than in a part of the filament that contains no other

phosphorylated NF-M proteins. Such cooperativity could be due to differences in the binding affinity of kinases to neurofilaments depending on their phosphorylation state. Alternatively, it is possible that neurofilament phosphorylation is regulated directly in response to some hypothetical spatial cue. One possible function of such regulation could be to locally regulate the interactions or space filling properties of neurofilaments. For example, neurofilaments can interact with microtubules in a dephosphorylation-dependent manner in vitro (Hisanaga and Hirokawa, 1990). In addition, a number of laboratories have reported a relationship between neurofilament phosphorylation and inter-neurofilament distance in vivo, though some evidence indicates that heavily phosphorylated neurofilaments are spaced more closely (Gotow and Tanaka, 1994; Gotow et al., 1994; Pijak et al., 1996; Szaro et al., 1990) and other evidence suggests that they are spaced further apart (de Waegh et al., 1992; Nixon et al., 1994).

Another question raised by the pattern of phosphorylation observed in this paper is the extent to which it applies to other phosphorylation sites within the tail domain of NF-M, and also NF-H. There are six different sites that are phosphorylated within the tail domain of NF-M in vivo (Xu et al., 1992) but the epitopes that the RMO55 and FNP7 antibodies bind to have not been localized. In principle, it is possible that these antibodies could bind to different phosphorylation states of the same epitope, though it would seem more likely that they bind to different epitopes because RMO55 does not cross-react with NF-H whereas FNP7 does. If contiguous phosphorylated and non-phosphorylated domains along individual neurofilaments do exist at more than one phosphorylation site, then do these domains coincide or do they overlap? To address this question with the indirect immunofluorescence protocol used here is difficult because both RMO55 and FNP7 are derived from mice, but this question could be addressed readily by conjugating fluorophore directly to these antibodies and performing direct immunofluorescence, or by using phosphorylation-dependent antibodies from different host species.

I am very grateful to Dr Virginia Lee of the University of Pennsylvania for providing me with the monoclonal and polyclonal antibodies used in this work and for her helpful advice. This work was supported by a grant from the National Institutes of Health.

REFERENCES

- Archer, D. R., Watson, D. F. and Griffin, J. W. (1994). Phosphorylation-dependent immunoreactivity of neurofilaments and the rate of slow axonal transport in the central and peripheral axons of the rat dorsal root ganglion. *J. Neurochem.* **62**, 1119-1125.
- Baas, P. W. and Black, M. M. (1990). Individual microtubules in the axon consist of domains that differ in both composition and stability. *J. Cell Biol.* **111**, 495-509.
- Bennett, G. S., Tapscott, S. J., DiLullo, C. and Holtzer, H. (1984). Differential binding of antibodies against the neurofilament triplet proteins in different avian neurons. *Brain Res.* **304**, 291-302.
- Bennett, G. S. and DiLullo, C. (1985). Slow post-translational modification of a neurofilament protein. *J. Cell Biol.* **100**, 1799-1804.
- Benson, D. L., Mandell, J. W., Shaw, G. and Banker, G. (1996). Compartmentation of alpha-internexin and neurofilament triplet proteins in cultured hippocampal neurons. *J. Neurocytol.* **25**, 181-196.
- Black, M. M., Keyser, P. and Sobel, E. (1986). Interval between the synthesis

- and assembly of cytoskeletal proteins in cultured neurons. *J. Neurosci.* **6**, 1004-1012.
- Black, M. M., Slaughter, T. and Fischer, I.** (1994). Microtubule-associated protein 1b (MAP1b) is concentrated in the distal region of growing axons. *J. Neurosci.* **14**, 857-870.
- Bottenstein, J. E. and Sato, G. H.** (1979). Growth of a rat neuroblastoma cell line in serum-free supplemented media. *Proc. Nat. Acad. Sci. USA* **76**, 514-517.
- Brown, A., Slaughter, T. and Black, M. M.** (1992). Newly assembled microtubules are concentrated in the proximal and distal regions of growing axons. *J. Cell Biol.* **119**, 867-882.
- Brown, A., Li, Y., Slaughter, T. and Black, M. M.** (1993). Composite microtubules of the axon: quantitative analysis of tyrosinated and acetylated tubulin along individual axonal microtubules. *J. Cell Sci.* **104**, 339-352.
- Brown, A.** (1997). Visualization of single neurofilaments by immunofluorescence microscopy of splayed axonal cytoskeletons. *Cell Motil. Cytoskel.* **38**, 133-145.
- Carden, M. J., Schlaepfer, W. W. and Lee, V. M.** (1985). The structure, biochemical properties, and immunogenicity of neurofilament peripheral regions are determined by phosphorylation state. *J. Biol. Chem.* **260**, 9805-9817.
- Carden, M. J., Trojanowski, J. Q., Schlaepfer, W. W. and Lee, V. M.** (1987). Two-stage expression of neurofilament polypeptides during rat neurogenesis with early establishment of adult phosphorylation patterns. *J. Neurosci.* **7**, 3489-3504.
- Chin, T. K., Harding, S. E. and Eagles, P. A. M.** (1989). Characterization of two proteolytically derived soluble polypeptides from the neurofilament triplet components NFM and NFH. *Biochem. J.* **264**, 53-60.
- Ching, G. Y. and Liem, R. K.** (1993). Assembly of type IV neuronal intermediate filaments in nonneuronal cells in the absence of preexisting cytoplasmic intermediate filaments. *J. Cell Biol.* **122**, 1323-1335.
- Cleveland, D. W., Monteiro, M. J., Wong, P. C., Gill, S. R., Gearhart, J. D. and Hoffman, P. N.** (1991). Involvement of neurofilaments in the radial growth of axons. *J. Cell Sci. Suppl.* **15**, 85-95.
- Cochard, P. and Paulin, D.** (1984). Initial expression of neurofilaments and vimentin in the central and peripheral nervous system of the mouse embryo in vivo. *J. Neurosci.* **4**, 2080-2094.
- de Waegh, S. M., Lee, V. M. and Brady, S. T.** (1992). Local modulation of neurofilament phosphorylation, axonal caliber, and slow axonal transport by myelinating Schwann cells. *Cell* **68**, 451-463.
- Eagles, P. A. M., Pant, H. C. and Gainer, H.** (1990). Neurofilaments. In *Cellular and Molecular Biology of Intermediate Filaments* (ed. R. D. G. P. M. Steinert), pp. 37-94. Plenum Publishing Corporation, New York.
- Elhanany, E., Jaffe, H., Link, W. T., Sheeley, D. M., Gainer, H. and Pant, H. C.** (1994). Identification of endogenously phosphorylated KSP sites in the high-molecular-weight rat neurofilament protein. *J. Neurochem.* **63**, 2324-2335.
- Foster, G. A., Dahl, D. and Lee, V. M.** (1987). Temporal and topographic relationships between the phosphorylated and nonphosphorylated epitopes of the 200 kDa neurofilament protein during development in vitro. *J. Neurosci.* **7**, 2651-2663.
- Georges, E., Lefebvre, S. and Mushynski, W. E.** (1986). Dephosphorylation of neurofilaments by exogenous phosphatases has no effect on reassembly of subunits. *J. Neurochem.* **47**, 477-483.
- Georges, E. and Mushynski, W. E.** (1987). Chemical modification of charged amino acid moieties alters the electrophoretic mobilities of neurofilament subunits on SDS/polyacrylamide gels. *Eur. J. Biochem.* **165**, 281-287.
- Gotow, T. and Tanaka, J.** (1994). Phosphorylation of neurofilament H subunit as related to arrangement of neurofilaments. *J. Neurosci. Res.* **37**, 691-713.
- Gotow, T., Tanaka, T., Nakamura, Y. and Takeda, M.** (1994). Dephosphorylation of the largest neurofilament subunit protein influences the structure of crossbridges in reassembled neurofilaments. *J. Cell Sci.* **107**, 1949-1957.
- Harris, J., Ayyub, C. and Shaw, G.** (1991). A molecular dissection of the carboxyterminal tails of the major neurofilament subunits NF-M and NF-H. *J. Neurosci. Res.* **30**, 47-62.
- Hisanaga, S. and Hirokawa, N.** (1989). The effects of dephosphorylation on the structure of the projections of neurofilament. *J. Neurosci.* **9**, 959-966.
- Hisanaga, S., Gonda, Y., Inagaki, M., Ikai, A. and Hirokawa, N.** (1990). Effects of phosphorylation of the neurofilament L-protein on filamentous structures. *Cell Reg.* **1**, 237-248.
- Hisanaga, S. and Hirokawa, N.** (1990). Dephosphorylation-induced interactions of neurofilaments with microtubules. *J. Biol. Chem.* **265**, 21852-21858.
- Hisanaga, S., Yasugawa, S., Yamakawa, T., Miyamoto, E., Ikebe, M., Uchiyama, M. and Kishimoto, T.** (1993). Dephosphorylation of microtubule-binding sites at the neurofilament-H tail domain by alkaline, acid and protein phosphatases. *J. Biochem.* **113**, 705-709.
- Hisanaga, S., Matsuoka, Y., Nishizawa, K., Saito, T., Inagaki, M. and Hirokawa, N.** (1994). Phosphorylation of native and reassembled neurofilaments composed of NF-L, NF-M, and NF-H by the catalytic subunit of cAMP-dependent protein kinase. *Mol. Biol. Cell* **5**, 161-172.
- Julien, J.-P. and Mushynski, W. E.** (1983). The distribution of phosphorylation sites among identified proteolytic fragments of mammalian neurofilaments. *J. Biol. Chem.* **258**, 4019-4025.
- Landmesser, L. and Swain, S.** (1992). Temporal and spatial modulation of a cytoskeletal antigen during peripheral axonal pathfinding. *Neuron* **8**, 291-305.
- Lee, M. K., Xu, Z., Wong, P. C. and Cleveland, D. W.** (1993). Neurofilaments are obligate heteropolymers in vivo. *J. Cell Biol.* **122**, 1337-1350.
- Lee, M. K. and Cleveland, D. W.** (1996). Neuronal intermediate filaments. *Annu. Rev. Neurosci.* **19**, 187-217.
- Lee, V. M.** (1985). Neurofilament protein abnormalities in PC12 cells: comparison with neurofilament proteins of normal cultured rat sympathetic neurons. *J. Neurosci.* **5**, 3039-3046.
- Lee, V. M., Carden, M. J. and Trojanowski, J. Q.** (1986). Novel monoclonal antibodies provide evidence for the in situ existence of a nonphosphorylated form of the largest neurofilament subunit. *J. Neurosci.* **6**, 850-858.
- Lee, V. M., Carden, M. J., Schlaepfer, W. W. and Trojanowski, J. Q.** (1987). Monoclonal antibodies distinguish several differentially phosphorylated states of the two largest rat neurofilament subunits (NF-H and NF-M) and demonstrate their existence in the normal nervous system of adult rats. *J. Neurosci.* **7**, 3474-3488.
- Li, Y. and Black, M. M.** (1996). Microtubule assembly and turnover in growing axons. *J. Neurosci.* **16**, 531-544.
- Mandell, J. W. and Banker, G. A.** (1996). A spatial gradient of tau protein phosphorylation in nascent axons. *J. Neurosci.* **16**, 5727-5740.
- Mata, M., Kupina, N. and Fink, D. J.** (1992). Phosphorylation-dependent neurofilament epitopes are reduced at the node of Ranvier. *J. Neurocytol.* **21**, 199-210.
- Nixon, R. A. and Lewis, S. E.** (1986). Differential turnover of phosphate groups on neurofilament subunits in mammalian neurons in vivo. *J. Biol. Chem.* **261**, 16298-16301.
- Nixon, R. A., Lewis, S. E. and Marotta, C. A.** (1987). Post-translational modification of neurofilament proteins by phosphate during axoplasmic transport in retinal ganglion cell neurons. *J. Neurosci.* **7**, 1145-1158.
- Nixon, R. A. and Sihag, R. K.** (1991). Neurofilament phosphorylation: a new look at regulation and function. *Trends Neurosci.* **14**, 501-506.
- Nixon, R. A., Paskevich, P. A., Sihag, R. K. and Thayer, C. Y.** (1994). Phosphorylation on carboxyl terminus domains of neurofilament proteins in retinal ganglion cell neurons in vivo: Influences on regional neurofilament accumulation, interneurofilament spacing, and axon caliber. *J. Cell Biol.* **126**, 1031-1046.
- Oblinger, M.** (1987). Characterization of the post-translational modification of the mammalian high molecular weight neurofilament protein in vivo. *J. Neurosci.* **7**, 2510-2521.
- Pachter, J. S. and Liem, R. K. H.** (1984). The differential appearance of neurofilament triplet polypeptides in the developing rat optic nerve. *Dev. Biol.* **103**, 200-210.
- Pant, H. C. and Veeranna** (1995). Neurofilament phosphorylation. *Biochem. Cell Biol.* **73**, 575-592.
- Pijak, D. S., Hall, G. F., Tenicki, P. J., Boulos, A. S., Lurie, D. I. and Selzer, M. E.** (1996). Neurofilament spacing, phosphorylation, and axon diameter in regenerating and uninjured lamprey axons. *J. Comp. Neurol.* **368**, 569-581.
- Riederer, B. M., Porchet, R. and Marugg, R. A.** (1996). Differential expression and modification of neurofilament triplet proteins during cat cerebellar development. *J. Comp. Neurol.* **364**, 704-717.
- Rochlin, M. W., Wickline, K. M. and Bridgman, P. C.** (1996). Microtubule stability decreases axon elongation but not axoplasm production. *J. Neurosci.* **16**, 3236-3246.
- Saito, T., Shima, H., Osawa, Y., Nagao, M., Hemmings, B., Kishimoto, T. and Hisanaga, S.** (1995). Neurofilament-associated protein phosphatase 2A: its possible role in preserving neurofilaments in filamentous states. *Biochemistry* **34**, 7376-7384.

- Shaw, G. and Weber, K.** (1982). Differential appearance of neurofilament triplet proteins in brain development. *Nature* **298**, 277-279.
- Shaw, G., Banker, G. A. and Weber, K.** (1985). An immunofluorescence study of neurofilament protein expression by developing hippocampal neurons in tissue culture. *Eur. J. Cell Biol.* **39**, 205-216.
- Shaw, G.** (1991). Neurofilament proteins. In *The Neuronal Cytoskeleton* (ed. R. D. Burgoyne), pp. 183-212. Wiley-Liss, Inc., New York, NY.
- Slaughter, T., Wang, J. and Black, M. M.** (1997). Microtubule transport from the cell body into the axons of growing neurons. *J. Neurosci.* **17**, 5807-5819.
- Starr, R., Attema, B., DeVries, G. H. and Monteiro, M. J.** (1996). Neurofilament phosphorylation is modulated by myelination. *J. Neurosci. Res.* **44**, 328-337.
- Sternberger, L. A. and Sternberger, N. H.** (1983). Monoclonal antibodies distinguish phosphorylated and nonphosphorylated forms of neurofilaments in situ. *Proc. Nat. Acad. Sci. USA* **80**, 6126-6130.
- Szaro, B., Lee, V. and Gainer, H.** (1989). Spatial and temporal expression of phosphorylated and non-phosphorylated forms of the neurofilament proteins in the developing nervous system of *Xenopus laevis*. *Dev. Brain Res.* **48**, 87-103.
- Szaro, B. G., Whitnall, M. H. and Gainer, H.** (1990). Phosphorylation-dependent epitopes on neurofilament proteins and neurofilament densities differ in axons in the corticospinal and primary sensory dorsal column tracts in the rat spinal cord. *J. Comp. Neurol.* **302**, 220-235.
- Trojanowski, J. Q., Kelsten, M. L. and Lee, V. M.-Y.** (1989). Phosphate-dependent and independent neurofilament protein epitopes are expressed throughout the cell cycle in human medulloblastoma (D283 MED) cells. *Am. J. Pathol.* **135**, 747-758.
- Veeranna, Sheety, K. T., Link, W. T., Jaffe, H., Wang, J. and Pant, H. C.** (1995). Neuronal cyclin-dependent kinase-5 phosphorylation sites in neurofilament protein (NF-H) are dephosphorylated by protein phosphatase 2A. *J. Neurochem.* **64**, 2681-2690.
- Xu, Z. S., Liu, W. S. and Willard, M. B.** (1992). Identification of six phosphorylation sites in the COOH-terminal tail region of the rat neurofilament protein M. *J. Biol. Chem.* **267**, 4467-4471.